Quantum-mechanical approach to the laser-assisted vacuum decay

Q. Z. Lv, S. Dong, C. Lisowski, R. Pelphrey, Y. T. Li, Q. Su, and R. Grobe

Phys. Rev. A **97**, 053416 — Published 30 May 2018

DOI: 10.1103/PhysRevA.97.053416

Quantum mechanical approach to the laser-assisted vacuum decay

Q.Z. Lv[1,2], S. Dong[4,5], C. Lisowski[4], R. Pelphrey[4], Y.T. Li[2,3], Q. Su[4] and R. Grobe[4]

(1) Max-Planck-Institut für Kernphysik, Saupfercheckweg 1, 69117 Heidelberg, Germany

(2) Beijing National Laboratory for Condensed Matter Physics, Institute of Physics
Chinese Academy of Sciences, Beijing 100190, China

(3) School of Physical Sciences, University of Chinese Academy of Sciences,
Beijing 100049, China

(4) Intense Laser Physics Theory Unit and Department of Physics
Illinois State University, Normal, IL 61790-4560, USA

(5) School of Physics and Astronomy, Collaborative Innovation Center of IFSA,
Shanghai Jiao Tong University, Shanghai 200240, China

The quantum field theoretical problem of the vacuum decay into electron-positron pairs induced by external force fields is mapped onto the framework of a quantum mechanical scattering process. This mapping permits us to generalize the Hund conjecture, which relates the long-time pair creation rate for a static and spatially localized electric field to the transmission coefficient, to general space-time dependent forces that can induce multi-photon transitions. This leads to conceptual as well as computational simplifications as the vacuum's decay rate can be obtained from the laser-assisted scattering of quantum mechanical wave packets. Using this mapping we find an analytical expression for the pair creation rate for the case where the laser's polarization direction is perpendicular to the supercritical static force field.

As the result of the recent advances in the development of new light sources with unprecedented high intensities [1], the possibility to probe the instability of the quantum electrodynamical vacuum state with external fields has found a considerable interest [2]. There are two intrinsically different mechanisms by which electron-positron pairs can be created from the vacuum. The first scheme [3] requires the field (which can be static) to be extremely large and can be visualized in terms of a tunneling process between energy shifted Dirac states, while the second scheme [4,5] creates particles through single- or multi-photon processes by requiring a time-dependent field with a large frequency.

Numerous theoretical approaches to study the pair-creation are based on the observation that the quantum field theoretical expectation value of the electric current density (which is given by a commutator of the field operators associated with charge symmetrization) can be related to a Green's function and therefore to an action integral [3]. Alternatively, and more relevant to this work, one can study the dynamics also from a space-time resolved perspective, where solutions to the time-dependent Dirac equation for a set of suitable initial states are usually examined [6].

In a pioneering work in 1940, F. Hund [7] examined quantum mechanically as well as quantum field theoretically the stationary processes associated with a single and double step potential barrier with a height $|V_0|$ that exceeds $2mc^2/|q|$, where m and q are the electron's mass and charge and c is the speed of light. He conjectured that the matter creation rate for such a supercritical potential configuration can be obtained from the simple ratio of the transmitted and incoming current densities. This conjecture opened the door to calculate the pair creation rate Γ for time-independent potentials with arbitrary spatial dependence from the energy integral of the corresponding quantum mechanical transmission coefficient T(E), i.e. $\Gamma = (2\pi)^{-1} \int dE\, T(E)$. This useful expression was employed in numerous works [8-12] to compute Γ for several time-independent electric field configurations, and recently it was also suggested that Hund's conjecture can even be applied to other combined static electric-magnetic configurations [13].

As recently the prospects of combining static and time-dependent fields to lower the critical field have triggered new discussions [2], it seems worthwhile to explore if Hund's conjecture to map an intrinsic quantum field theoretical process onto a quantum mechanical scattering problem could even be generalized to those external force fields that in addition to a spatial dependence have also a temporal dependence. If this is possible and the vacuum's decay rate can be calculated from the laser-assisted scattering system, then this quantum field theoretical process should also be

amenable to powerful solution techniques, such as the Kroll-Watson formula [14] and its generalizations [15-20] and other techniques that so successfully described laser-assisted scattering experiments [21-23].

The purpose of this work is actually three-fold. We will show first that the mapping of the quantum field theoretical pair creation problem onto a quantum mechanical scattering problem (Hund rule) can be even generalized to external force fields that have a time dependence. This provides a better visualization of the pair creation process as well as new computational techniques calculating the pair creation rate and energy spectra of the created particles. Second, we suggest that the polarization direction of the laser field relative to the direction of the supercritical static external field is crucially important for the pair creation yield. Third, triggered by recent works [24-26], which pointed out the importance of the magnetic field component for those pair creation processes that are solely triggered by a laser field, we show that if the laser simply assists the pair creation process in a supercritical static field, this magnetic component is not so crucial.

The paper is organized as follows. In Section 2 we introduce the model system based on the time-dependent Dirac equation. In Section 3 we derive rigorously from quantum field theory how the vacuum's decay in a static supercritical potential can be mapped onto a quantum mechanical scattering problem. In Section 4 we generalize this mapping to the laser-assisted vacuum decay. In Section 5 we use this mapping to provide a remarkable accurate analytical expression for the laser-assisted vacuum decay rate for laser fields that are polarized perpendicular to the force direction associated with the supercritical static field. In Section 6 we examine the importance of the laser's magnetic field component. We close with a discussion of future problems in Section 7.

2. The model system

The four spinor components of the electron-positron quantum field operator $\Psi(\mathbf{r},t)$ fulfill the Dirac equation, $i\hbar\,\partial\Psi/\partial t = H\Psi$, where the interaction of the vacuum with the electromagnetic field [given by vector potential $\mathbf{A}(\mathbf{r},t) \equiv (A_x,A_y,A_z)$ and the scalar potential $V(\mathbf{r},t)$] is described by the Dirac Hamiltonian [27]

$$H = c\,\boldsymbol{\alpha}\,[\mathbf{p} - q\mathbf{A}(\mathbf{r},t)/c] + mc^2\,\beta + qV(\mathbf{r},t) \qquad (2.1)$$

where $\boldsymbol{\alpha} \equiv (\alpha_1, \alpha_2, \alpha_3)$ and β denote the set of the four 4×4 Dirac matrices. We use for our

calculation atomic units [28,29], where m=1, q= –1, ħ=1 and c=137.036. If the scalar potential $V(\mathbf{r},t)$ and vector potential $A(\mathbf{r},t)$ depend only on the coordinate x, the canonical momenta p_y and p_z are conserved. For simplicity, we focus on p_y=0, p_z=0, which simplifies the computational analysis significantly. Furthermore, as we will examine in this work linear polarized laser fields whose magnetic field component $\nabla\times\mathbf{A}(\mathbf{r},t)$ points in the z-direction, and we choose the spin aligned along the z-direction. We can still choose if the laser's polarization (electric field) points along the x- or y-direction. As the spin's direction is conserved, only two of the four spinor components are really required to describe the dynamics. Choosing A_z=0, the effective Hamiltonian for the two relevant spinor components of the field operator is given by

$$H = c\,\sigma_1\,p_x + \sigma_1\,A_x(x,t) + \sigma_2\,A_y(x,t) + mc^2\,\sigma_3 - V(x,t)\,\sigma_0 \qquad (2.2)$$

where σ_i (with i=0,1,2,3) denote the set of the four 2×2 Pauli matrices that satisfy the anti-commutation relations $\{\sigma_i,\sigma_j\} = 2\,i\,\delta_{i,j}$. For better clarity with regard to the concept of a radiative mass introduced in Sec. 5, we keep the mass m (=1.a.u.) in all expressions.

For the static part of the external force, we choose an electric field that points along the x-direction and is spatially localized along the x-direction. It is modeled by the Sauter [30] potential $V(x) = V_0\,[\tanh(x/w)–1]/2$, where w denotes the spatial extension of the electric field, given by $\mathbf{E}(x) = –\nabla V(x)$. For our analysis, we chose below a negative amplitude $V_0 = –2.5\,mc^2$, such that the corresponding electric field is negative and would accelerate an electron towards the positive-x direction.

The initial vacuum state is represented by the set of occupied eigenstates $|k;d\rangle$ of the (field-free) Dirac operator H_0 [$= c\,\sigma_1\,p_x + mc^2\sigma_3$] with negative energy that satisfy $H_0|k;d\rangle = -[m^2c^4+c^2k^2]^{1/2}\,|k;d\rangle$. We assume that our system has a finite spatial extension L and that all states satisfy periodic boundary conditions. As a result, the states can be normalized as $\langle k_1;d|k_2;d\rangle = \delta_{k1,k2}$ and they have a momentum mode spacing $\Delta k=2\pi/L$. The corresponding positive-energy states with momentum p are denoted by $|p;u\rangle$. In computational quantum field theory [28] the required space-time evolution of the electron-positron quantum field operator can be obtained equivalently from the time evolution of the set of all states $|k;d\rangle$ and the resulting matrix elements $U_{pk}(t) \equiv \langle p;u|U(t)|k;d\rangle$, where U(t) is the time-ordered evolution operator associated with H. The solutions of the space-time

dependent Dirac equation with the external potentials $\mathbf{A}(x,t)$ and $V(x,t)$ can be obtained on a space-time lattice with N_t temporal and N_x spatial grid points using efficient fast-Fourier transformation based split-operator schemes [31-33]. The total number of created electron-positron pairs after the interaction at final time t is then obtained from all time-evolved Hilbert-space states as $N(t) \equiv \Sigma_{p,k} |U_{pk}(t)|^2$. As the calculation of this particle number is based on the projection on the field-free states, a direct interpretation of N(t) during the interaction time is non-trivial. For example, if the external field is supercritical, then it is not even possible to distinguish between positively and negatively charged particles inside the interaction zone. The corresponding matrix elements are also gauge invariant [34].

This expression, derived from quantum field theory, permits us also to calculate the *number density* of the created positrons $N_k(t)$ with a particular (discrete) momentum k. Following the traditional hole theory, the dynamically induced depletion rate of a particular negative energy state $|k;d\rangle$ (with negative energy E_{neg} and momentum k) to states with positive energy is identical to the creation rate of a positron with the final (positive) energy $E=|E_{neg}| \equiv [m^2c^4+c^2k^2]^{1/2}$. This interpretation suggests that the momentum distribution after the interaction at final time t is then given by the sum over all final states $|p;u\rangle$ that have a positive energy

$$N_k(t) \equiv \Sigma_p |U_{pk}(t)|^2 \tag{2.3}$$

Using this (discrete) momentum density $N_k(t)$ we can also define a (continuous) energy density associated with the continuum limit where the box size $L\rightarrow\infty$ and the discrete summations over k become integrations. For example, the total number of created positrons can be expressed as an energy integral, i.e., $N(t) = \Sigma_k N_k(t) \equiv \int dE\, N(E,t)$. If we replace the discrete summation by an energy integral, i.e., $\Sigma_k \rightarrow (\Delta k)^{-1} \int dk = L/(2\pi) \int dk = L/(2\pi) \int dE/v$, where v denotes the velocity $v=dE/dk=c^2k\,[m^2c^4+c^2k^2]^{-1/2}$, we obtain

$$N(E,t) = N_k(t)\, L/(2\pi)/v \tag{2.4}$$

We should point out that the final energy spectrum of the created electrons and positrons do not necessarily match as the two charges are mainly ejected in opposite spatial directions and their final

spectra can also be affected by possible after-accelerations due to the consecutive interaction with localized additional (weaker) force fields that are spatially accessible to only one type of particle species.

Formally, the energy spectrum of the electrons is obtained from the sum over all absolute value squared transition elements to a specific positive energy state $|p;u\rangle$ originating from *all* possible Dirac sea states $|k;d\rangle$ with the final (positive) energy $E = [m^2c^4+c^2p^2]^{1/2}$, i.e. $N_p(t) \equiv \Sigma_k |U_{pk}(t)|^2$. Equivalently, for consistency, the same energy spectrum could be obtained from the corresponding charge-conjugated hole theory, in which the initial Dirac state $|p;d\rangle$ is evolved under the Hamiltonian H(-q), such that here the depletion of the state $|p;d\rangle$ to all states $|k;u\rangle$ corresponds to the creation of an *electron* with energy $E = [m^2c^4+c^2p^2]^{1/2}$.

The fact that the spectra of the two-particle species do not agree in general does not violate the conservation of the total charge, as the total number of created positrons, $N(t) = \Sigma_k N_k(t) = \Sigma_p N_p(t)$, matches for both expressions of $N_k(t)$ and $N_p(t)$, i.e., $N(t) = \Sigma_k \Sigma_p |U_{pk}(t)|^2$. We also point out that these quantum field theoretical predictions cannot describe the correlations between the two energies within a single detected electron-positron pair.

It turns out, however, there are some specific electromagnetic field configurations, for which the electrons' and positrons' energy spectra can be identical. For example, if the static potential in the Hamiltonian $H(q) = c\,\sigma_1\,p_x + mc^2\,\sigma_3 + qV(x,t)\,\sigma_0$ has the spatial symmetry $V(x) = -V(-x)$, then there exits a space-inversion operator P such that $P\,H(q)\,P = H(-q)$. Here the space-inversion matrix operator is defined as $\mathbf{P = \sigma_3\,p}$, where **p** reverses the position argument, i.e., $\mathbf{p}\,F(x) = F(-x)$.

The proof for identical energy spectra in this case is straightforward. We can first insert the unit operator P^2 into the transition matrix elements, using the symmetry of H(q) and the property $P\,\langle x|k;d\rangle = \langle x|-k;d\rangle$ and $P\,\langle x|p;u\rangle = \langle x|-p;u\rangle$ we obtain

$$N_k(t) = \Sigma_p |U_{pk}(t)|^2 = \Sigma_p |\langle p;u|\, P^2 Exp[\,-i\,H(q)\,t]\,P^2\,|k;d\rangle|^2$$
$$= \Sigma_p |\langle -p;u|\, Exp[\,-i\,H(-q)\,t]\,|-k;d\rangle|^2 \qquad (2.1)$$

This expression is obviously the energy density of a created *electron* derived from a hole theory with a positronic Dirac sea, governed by H(-q). Here the depletion of the state $|-k;d\rangle$ under the positronic Hamiltonian H(-q) corresponds to the creation of an electron with energy E=

$[m^2c^4+c^2(-k)^2]^{1/2}$.

3. Pair creation due to a supercritical static force field given by V(r)

In Sec. 3.1 we derive how the quantum field theoretical problem of determining the time-dependence of the number of created positrons with a given energy E can be mapped onto a single-particle quantum mechanical scattering problem. In Sec. 3.2 we provide a concrete numerical example of the space-time evolution of a (spatially infinitely extended) Dirac sea state. In Sec. 3.3 we examine the corresponding evolution of a spatially localized wave packet.

3.1 Mapping of the vacuum decay onto a scattering problem

Let us discuss two properties of the time-dependent energy density N(E,t) of the created positrons. We will use Eq. (2.3) and (2.4), where N(E,t) can be computed from the depletion dynamics of a *single* Dirac state. First, we will show that for any interaction, N(E,t) can be obtained from the spatially integrated density of certain wave function solutions of the Dirac equation. This relationship will permit us a convenient space-time resolved interpretation of the pair creation process and also guide us to derive the quantum mechanical means to compute the pair creation yields for more complicated cases where the static force field is accompanied by a time-dependent field.

First, using the normalization $\langle p_2;u|p_1;u\rangle = \delta_{p1,p2}$ we insert the unit-operator expressed as the integration over all position eigenstates $1 = \int dx\ |x\rangle\langle x|$ into the expression for $N_k(t)$. Here the spatial integration extends over the length L of the system. As a result, $N_k(t)$ can be interpreted as a spatial integral [area under $\rho_k(x,t)$]

$$\begin{aligned} N_k(t) \equiv \Sigma_p\, |U_{pk}(t)|^2 &= \Sigma_{p1}\, \Sigma_{p2}\, \langle p_2;u|p_1;u\rangle\, U_{p1k}(t)\, U_{p2k}(t)^* \\ &= \int dx\ \Sigma_{p1}\, \Sigma_{p2}\, \langle p_2;u|x\rangle\langle x|p_1;u\rangle\, U_{p1k}(t)\, U_{p2k}(t)^* \\ &= \int dx\ \left|\Sigma_p\, U_{pk}(t)\, \langle x|p;u\rangle\right|^2 \\ &\equiv \int dx\ \rho_k(x,t) \end{aligned} \tag{3.2}$$

The positive space-time dependent function $\rho_k(x,t)$ defined as $\left|\Sigma_p\, U_{pk}(t)\, \langle x|p;u\rangle\right|^2$ with E= $[m^2c^4+c^2k^2]^{1/2}$ deserves special attention. It is the spatial density associated with the *positive*

energy portion of the state $|k;d(t)\rangle \equiv U(t)\,|k;d\rangle$, evolved under the full Dirac Hamiltonian containing V(x,t) and **A**(x,t). This can be easily seen by employing the projection operator into the positive energy manifold $\Sigma_p\,|p;u\rangle\langle p;u|$, while $\Sigma_p\,|p;u\rangle\langle p;u| + \Sigma_k\,|k;d\rangle\langle k;d|$ is the unit operator in this notation:

$$\rho_k(x,t) \equiv \left|\Sigma_p\ U_{pk}(t)\,\langle x|p;u\rangle\right|^2 = \left|\langle x|\ \Sigma_p\,|p;u\rangle\,U_{pk}(t)\right|^2 = \left|\langle x|\ \Sigma_p\,|p;u\rangle\langle p;u|\ k;d(t)\rangle\right|^2 \qquad (3.3)$$

While the initial state $|k;d\rangle$ is spatially infinitely extended, the density $\rho_k(x,t)$ evolves from zero and its area $\int dx\ \rho_k(x,t)$ is equal to $N_k(t)$, which permits therefore a simple *quantum mechanical* interpretation of the pair creation process.

For the special case where the external field is time-independent, we show in Appendix A that N(E,t) grows (in the long-time limit) linearly in time with a rate that can be computed from the quantum mechanical transmission coefficient associated with the corresponding scattering situation. This second step will also provide a rigorous proof of the Hund conjecture based on quantum field theory. In Appendix B we show that if the electric field is symmetric with regard to a space inversion, the positrons' energy spectra is not only identical to the electrons' density, but it is also symmetric with regard to $|V_0|/2$. For the special case of an electric field that is spatially constant in a certain region, this rate matches well with the rate from Schwinger's calculation [35,36,37].

3.2 Time evolution of a single Dirac sea state

We will now illustrate the general finding above for a concrete numerical example. We choose the Sauter potential V(x) with a supercritical amplitude $V_0 = -2.5mc^2$ and w=0.3/c, and examine the temporal evolution of a single Dirac sea state $|k;d\rangle$ under the influence of V(x). The spatial representation of this initial 2-spinor state [before the interaction with V(x)] is given by $\langle x|k;d\rangle = N\,\{-k,\ c+(c^2+k^2)^{1/2}\}\,\exp(ikx)$, where N is the normalization factor chosen such that the density satisfies $\int dx\,|\langle x|k;d\rangle|^2 = 1$, with the integration limits –L/2and L/2. If we chose a negative momentum of $k = -[(E-|V_0|)^2 - m^2c^4]^{1/2}/c$ together with the parameter $E=1.25\ mc^2$, this amounts to k= –102.8 a.u. As a side note, we remark that this state $|k;d\rangle$ would be an energy eigenstate of the force-free Hamiltonian H_0 with negative energy $-1.25\ mc^2$. For x<0 [under the barrier V(x)] it

would describe a particle with a positive velocity $v_{inc} = c^2\, k/E$ (= 82.24 a.u. = 0.6c). As we chose here the specific value $E=|V_0|/2$ we automatically also have $v_{tran} = v_{inc}$, associated with the velocity it has for $V(x)\neq 0$, corresponding to $x>0$. A simple analytical expression [30,33,38] [given below in Eq. (5.1)] predicts that for this energy $E=1.25mc^2$ the transmission coefficient takes the value $T(E) = 0.272332$.

In Figure 1 we analyze the temporal evolution of the initial Dirac sea state $|k;d\rangle$. For three moments in time, we compare the density $\left|\langle x|k;d(t)\rangle\right|^2$ with the physically relevant density $\rho_k(x,t)$, which is associated with the positive-energy portion of the state after the interaction with the field.

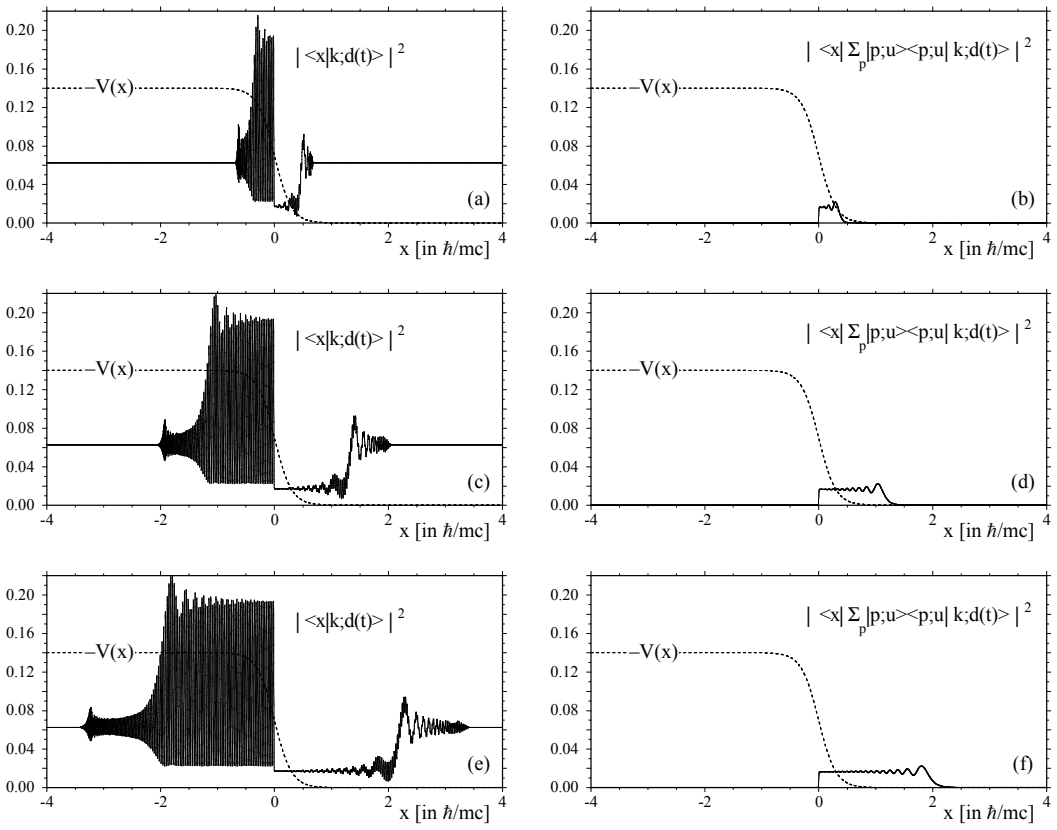

Figure 1 (a,c,e) Snapshots of the spatial density $|\langle x|k;d(t)\rangle|^2$ of a single initial state from the Dirac sea with $E=1.25mc^2$ and negative momentum k in the supercritical potential step at three moments in time (t_1=0.005a.u., t_2=0.015a.u., t_3=0.025a.u.) (b,d,f) The corresponding physical spatial probability density, associated with the state, but projected onto the positive energy manifold and given by $\rho_k(x,t) \equiv |\langle x|\,\Sigma_p\,|p;u\rangle\langle p;u|\,k;d(t)\rangle\,|^2$. As a reference, the dashed line is the shape of the supercritical potential energy $-V(x) = V_0\,[\tanh(x/w)-1]/2$.
(L= 16a.u., N_x=8192, N_t=6000, the interaction time was t=0.024 a.u.)

The two densities are already entirely different at the initial time t=0 before the interaction with V(x). While $\left|\langle x|k;d(t=0)\rangle\right|^2 = 1/L$ (=0.0625) is spatially constant over the entire extension L of our system, the initial density $\rho_k(x,t)$ vanishes due to the orthogonality $\langle p;u|\ k;d\rangle = 0$. As time evolves, the action of the force field triggers the generation of a reflected and transmitted part. The reflected portion originates close to x=0 and evolves with velocities $v_{refl} = -c^2\ |k|/[m^2c^4+c^2k^2]^{1/2}$ to the left. The original right traveling and reflected portions lead to strong interference patterns in $\left|\langle x|k;d(t)\rangle\right|^2$ as shown in Figs. 1a,c,e. The transmitted portion evolves to the right with velocity $v_{trans} = c^2\ p\ /[m^2c^4+c^2p^2]^{1/2}$ and momentum $p=(E^2-m^2c^4)^{1/2}/c$.

We point out that due to the unusual relationship between the momenta k and p for a given energy this is a very peculiar (non-classical and non-intuitive) scattering event. For a given energy an incoming particle with a small speed is *accelerated* and escapes to the right with a higher speed, whereas an incoming fast particle under the barrier emerges on the right side as a decelerated slower particle.

In more detail, the snapshot was taken after an interaction time of t = 0.025 a.u., during which a particle with the speed of light would move a characteristic distance of 3.4a.u. On the other hand, a particle evolving with a speed of v_{trans}=82.24 a.u. could only cover a distance of about 2 a.u. The complicated structures in $\left|\langle x|k;d\rangle\right|^2$ between 2 a.u. < |x| < 3.4 a.u. are therefore associated with states with very high negative energy excited during the abrupt turn-on of the potential.

On the left side, the oscillatory domain between -2a.u.< x < 0 a.u. is the result of the superposition between the incoming right- traveling state (with amplitude $1/L^{1/2}$ and velocity v_{inc} =82.24 a.u.) and the reflected portion (with amplitude $r(E)/L^{1/2}$ and velocity –82.24 a.u.), where the reflection coefficient is given by $r=[1-T(E)]^{1/2}$ amounting to r=0.853. As a result, the density can oscillate theoretically between $(1+r)^2/L$ (=0.215) and $(1-r)^2/L$ (=0.001), which matches roughly the observed amplitudes within our spatial resolution. The observed period of about 0.03 a.u. matches π/k, as expected. Finally, for the spatial range 0 a.u. < x < 2 a.u., we have only the transmitted portion with height T(E)/L (=0.0170), as the original density (with height 1/L) has vacated this area by moving to the right already to x>2. a.u.

In Figures 1b,d,f we display the density $\rho_k(x,t) \equiv \left|\langle x|\ \Sigma_p\ |p;u\rangle\langle p;u|\ k;d(t)\rangle\ \right|^2$, which is more

relevant for the pair creation process. Its structure is by far not as complicated as $\left|\langle x|k;d(t)\rangle\right|^2$. Due to the required projection $\Sigma_p\,|p;u\rangle\langle p;u|$ in the definition of $\rho_k(x,t)$, this density picks up only the truly transmitted portion. This transmitted portion corresponds precisely to the spatial probability density of the electrons created from the single Dirac sea state $|k;d\rangle$. We can read off the graph that its average height of $\rho_k(x,t)$ is 0.0170, which matches exactly the theoretically expected amplitude (derived in the appendices) and given by $|\tau(E)|^2/L$ where L (=16 a.u.) denotes the total length of our system. Note that because of $E=|V_0|/2$, we have here $|\tau(E)|^2= T(E)$. Furthermore, as time evolves, the area under the density grows linearly in time, $\int dx\, \rho_k(x,t) = 1.400\, t$, whose numerical value of the slope agrees again perfectly with the theoretically predicted value $1/L\ T(E)\ v_{inc}$, as derived in the appendices.

3.3 Time evolution of a wave packet

After analyzing the evolution of a single spatially delocalized Dirac state, let us now visualize the pair creation process in terms of a quantum mechanical wave packet scattering. In order to have a spatially localized wave packet, we superimpose several Dirac sea states according to

$$\phi(x,t=0) \equiv \Upsilon\, \Sigma_k \exp[\, ik_0x-(k-k_0)^2\, \Delta x_0{}^2] \,\langle x|k;d\rangle \qquad (3.4)$$

were the normalization factor Υ guarantees that $\int dx \left|\phi(x,t=0)\right|^2 =1$. If the momentum width of this wave packet is narrow enough such that the transmission coefficient is nearly constant over the narrow range of all incoming momenta, then this spatially localized state is a good approximation to the infinitely extended Dirac sea state with a sharp momentum. The density is centered around negative momentum k_0 and has a spatial width proportional to Δx_0. This state is localized initially under the barrier ($x_0<0$) and its center evolves to the force region, where part of it is transmitted to $x>0$. In the absence of the barrier, this state would take a *negative* central energy $-[m^2c^4+c^2k_0{}^2]^{1/2}$. However, as we have derived in Sec. 3.1, the energy that is relevant for the spectrum of the created positrons in the vacuum decay is actually *positive*, $E \equiv [m^2c^4+c^2k_0{}^2]^{1/2}$, which we denote by E from now on. To avoid any confusion, we note as a side issue, that (due to the presence of the barrier) the total energy of the wave packet amounts also to a total energy that is positive, $E_+ \equiv$

$|V_0|-[m^2c^4+c^2k_0^2]^{1/2}$, but this particular auxiliary energy is not directly relevant for the vacuum decay. Due to the energy conservation, these three energies are trivially related here. However, for the more general case, where the vacuum decay is assisted by a laser field, the total energy is not conserved. Here a single Dirac state (with momentum k) can evolve into a superposition of several states $|p;u\rangle$ with multiple energies, while the energy of the created positron remains determined solely by $[m^2c^4+c^2k^2]^{1/2}$.

In the limit of a large Δx_0, the area under the *final* transmitted portion, i.e.,

$$A_{fin}(E) \equiv \int_0^\infty dx \left|\phi(x,t)\right|^2 \qquad (3.5)$$

integrated from x=0 to x=∞, is identical to the transmission coefficient T(E) for each energy E. Therefore, according to Hund's conjecture, this transmitted probability portion is directly related to the pair-creation rate Γ(E) at that energy (multiplied with 2π), i.e. $2\pi\,\Gamma(E) = A_{fin}(E) = T(E)$

To test this conjecture numerically we have evolved the wave packet with Δx_0=0.3, k_0=–102.8 a.u., x_0=–1.2 a.u., corresponding to an energy E=1.25 mc^2 the same as in Sec. 3.2. After a time t=0.03 a.u. the area of the transmitted portion A_{fin} of the wave packet amounted to 0.2722 which matches the monoenergetic limit of $T(E=1.25mc^2)$. This illustrates again that we can determine the pair creation rate for a given energy either from the amplitude ($|\tau(k)|^2\ L^{-1}$) of an initial (infinitely extended) Dirac energy eigenstate (Sec. 3.2) or equivalently from the final area [$A_{fin}(E)$] of the transmitted wave packet. This observation will be important when we generalize this to the case (discussed below) where the pair creation process will be assisted by a time-dependent force.

4. Comparison of the vacuum decay with laser-assisted particle scattering

In this section, we will examine whether the mapping of the vacuum decay process onto a quantum mechanical scattering problem can be generalized if the pair creation due to the static supercritical field is assisted by a second force field that is time-dependent [35,39,40]. Due to the inherent non-stationarity of the process associated with the time-dependent force, it is non-trivial to define a transmission coefficient without any approximation, but we can still compare the process with the predictions for a scattered wave packet in the laser field.

We have examined two alternating but spatially homogenous electric fields that differ by their polarization direction relative to the static force (x-)direction of the supercritical field, corresponding to $\mathbf{E}(x,t) = E_0 \sin(\omega t)\, \mathbf{e_x}$ and $\mathbf{E}(x,t) = E_0 \sin(\omega t)\, \mathbf{e_y}$. This leads to the interaction potentials $A_x(x,t) = -E_0\ c \sin(\omega t)/\omega$ and similarly $A_y(x,t) = -E_0\ c \sin(\omega t)/\omega$ such that the two Hamiltonians read

$$H = c\, \sigma_1\, p_x + \sigma_1\, A_x(x,t)\, f(t) + mc^2\, \sigma_3 - V(x,t)\, \sigma_0 \qquad (4.1a)$$

$$H = c\, \sigma_1\, p_x + \sigma_2\, A_y(x,t)\, f(t) + mc^2\, \sigma_3 - V(x,t)\, \sigma_0 \qquad (4.1b)$$

The envelope f(t) was chosen to contain a very early time period of duration $2\times 2\pi/\omega$, where the laser was off. Using a $\sin^2$-pulse shape over one optical cycle, the laser was then turned on to its plateau value of f(t)=1. The turn-off follows the same sequence, but in reverse order. With regard to the parameters, we have chosen again $V_0=-2.5mc^2$ and w=0.3/c for the static field and $E_0=0.2c^3$ and $\omega=0.5mc^2$ for the time-dependent field. We note that the latter field is sufficiently small such that the number of created particle pairs solely associated with the alternating field (i.e. for $V_0=0$) is rather negligible. However, as we will see below, when the supercritical potential is present, the effect of this laser field onto the pair creation process is significant.

4.1 Generalization of a laser-modified rate for a non-monotonic growth of the yield

In Figure 2 we graph the temporal growth of the total number of created electrons N(t) for both laser field configurations. The laser was chosen spatially localized during the interaction around the location of the static supercritical field with a plateau-like envelope given by {Tanh[(x+d/2)/w] – Tanh[(x-d/2)/w]}/2 with an extension d = 0.3 a.u. and a spatial turn-on and off scale w = 5/c. During the early and later time of the interaction (when the field is slowly ramped up and down as described above) the growth of N(t) is mainly associated with the static potential, leading to a growth rate of about $\Gamma\approx 327$. This is fully consistent with the theoretical prediction from the energy integral over the transmission coefficient from mc^2 to $1.5\ mc^2$, which amounts to a numerical value $1/(2\pi) \int dE\ T(E) = 327.591$. We also observe that once the laser field has developed its maximum amplitude, the overall growth is *increased* for the case where $A_x \neq 0$ and *reduced* for $A_y \neq 0$. In addition, both data sets reveal superimposed heavy oscillations with constant amplitude. These

oscillations occur with frequency 2ω and are in phase with each other. The fact that these oscillations occur with a relatively *time-independent* amplitude suggests that it is possible to define an average linear growth rate even during the interaction, as indicated by the two parallel straight dashed lines in each figure. They have a slope of about 335 a.u. for $A_x \neq 0$ and about 231 for $A_y \neq 0$. As these average slopes [which we denote by $\Gamma(E_0, \omega)$] obviously determine the final electron-positron yield if the laser is turned off after a long time t, i.e. $N(t) = \Gamma(E_0, \omega)\, t$, it is possible to interpret from now on $\Gamma(E_0,\omega)$ as the laser-modified pair creation rate for this process. Obviously, in the special case of no laser field, $A_x=A_y=0$, it reduces to the original rate $\Gamma(E_0=0,\omega) = \Gamma$.

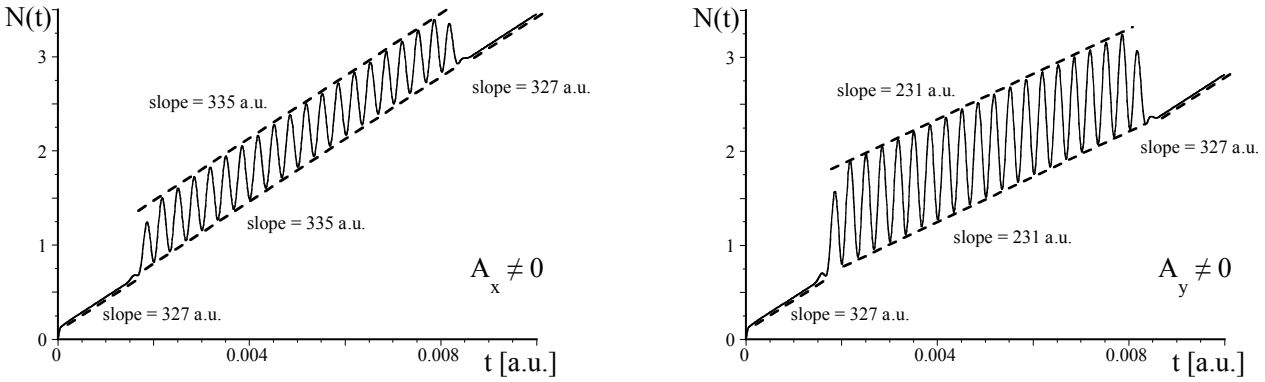

Figure 2 The number of created electron-positron pairs N(t) as a function of time. The pair-creation is assisted by a time-periodic field $\mathbf{A}(x,t) = -E_0\, c \sin(\omega t)/\omega\, \mathbf{e_x}$ or $\mathbf{A}(x,t) = -E_0\, c \sin(\omega t)/\omega\, \mathbf{e_y}$. For comparison, we provide dashed lines that have specified slopes.
($V_0 = 2.5mc^2$, $w=0.3/c$, $E_0 = 0.2c^3$, $\omega = 0.5mc^2$, $L= 3$a.u., $N_x=2048$, $N_t=18000$, laser field was turned on smoothly at time $t=2\times 2\pi/\omega$ ($=1.3\times10^{-3}$ a.u.) and off at time $t=12\times 2\pi/\omega$ ($=8.0\times10^{-3}$ a.u.) over one cycle of duration $2\pi/\omega$ ($=6.7\times10^{-4}$ a.u.) and with a 9-cycle plateau in between).

The amplitude of the oscillations during the interaction is not so relevant and simply reflects the dressing of the Dirac sea states due to the laser field. In fact, the amplitude increases directly with the spatial extension d of the laser pulse.

4.2 Laser-assisted scattering

In order to compare the pair-creation process with the quantum mechanical scattering also in the presence of the laser field, we have repeated in Fig. 3 the wave packet scattering simulations

described in the last part of Section 3. The wave packet has an initial location $x_0 = -1.5$ a.u. and $\Delta x_0 = 0.06$ and initial (negative) momentum k_0. In the absence of the potential barrier it would have a central energy that is negative with the magnitude $E = [m^2c^4 + c^2k_0^2]^{1/2}$. It was injected into the potential barrier (around x=0). The final area of the transmitted portion $A_{fin}(E)$ was calculated. The total simulation time was chosen sufficiently large for each incoming energy, such that the entire wave packet has scattered completely and A_{fin} becomes independent of time.

For comparison, the top pair of graphs (labeled A=0) in Figure 3 display the corresponding data for the dynamics in the absence of the laser field. Displayed are the final areas $A_{fin}(E)$ of the transmitted portion of the Gaussian wave packet as a function of the incoming energy (open circles), and also the scaled energy spectrum N(E,t) of the created positrons obtained from the quantum field theoretical simulation (continuous line). As the number of particles for a given energy increases monotonically with the interaction time, it had to be normalized, i.e. we have graphed $N(E,t)\ 2\pi/t$. At early times this spectrum is very wide in energy, but as the time increases only the part within the energy range $mc^2 < E < 1.5mc^2$ continues to grow. The agreement between the two data sets for each energy is excellent, so it illustrates numerically that $A_{fin}(E) = N(E,t)\ 2\pi/t$. Therefore, also the corresponding integral of $A_{fin}(E)$ over all energies reproduces correctly the observed vacuum decay rate Γ, i.e. $\Gamma = 1/(2\pi) \int dE\ A_{fin}(E)$.

The key question that we are interested in here is whether the numerical value of the energy integral $1/(2\pi) \int dE\ A_{fin}(E)$ is still related to the laser-assisted pair-creation rate $\Gamma(E_0,\omega)$.

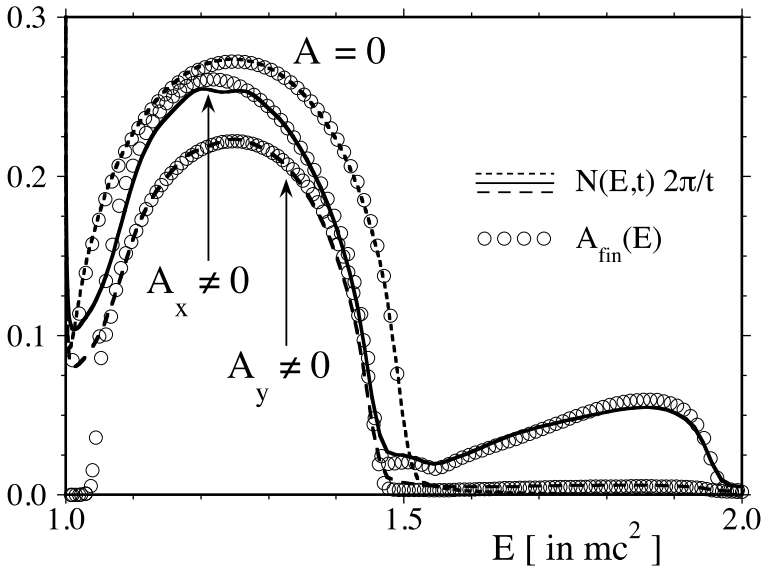

Figure 3 The three lines are the rescaled energy spectra of the created particles from the laser-assisted pair creation process, N(E,t) $2\pi/t$. The open circles are final areas $A_{fin}(E)$ of a transmitted Gaussian wave packet as a function of the incoming energy E. The particle that has been scattered off the supercritical potential V(x) in the presence of a time-periodic field $A(\mathbf{r},t) = -E_0\, c\, \sin(\omega t)/\omega$, pointing along either the x- or y-direction. (same parameters as in Fig. 2; for the scattering simulation we used L=20a.u., N_x=16384, N_t=18000, x_0=–1.5 a.u., Δx=0.0012, t = 9.5 x10^{-3}).

The next pair of data (labeled $A_x \neq 0$) is for the pair creation and scattering dynamics where the laser field is parallel to the supercritical static electric field. For small energies E<1.5 mc^2, there are fewer positrons created due the presence of the laser field, but at the same time the laser induces the creation of higher energetic positrons that could not be created solely by the static field. Most importantly, the energy spectrum of the created particles is matched again very well by the transmitted wave packet portion of the corresponding quantum mechanical scattering dynamics.

It is interesting to note that this field configuration permits the scattering event to be accompanied by the irreversible absorption and emission of photons. While incoming particle energies for E>$|V_0|$-mc^2 (=1.5mc^2) are outside the Klein tunneling region and therefore cannot be transmitted through the static barrier, the corresponding Dirac state can nevertheless become depleted as the emission of a photon lowers its energy into the permitted Klein tunneling region. Equivalently, one could argue that the large final energy of the created positron, E > 1.5mc^2, is due to the (permitted) absorption of a photon during the scattering process. We should point out again that the energy axis represents *both* the energy of the *outgoing* created positron as well as the absolute value of the (force-free and negative) energy of the scattered *incoming* particle. This is

relevant as, in contrast to the laser-free scattering, for $A_x \neq 0$ the energy of the scattered particle can change.

The lowest pair (labeled $A_y \neq 0$) corresponds to the data for the laser field perpendicular to the supercritical field. Here for each energy the number of created positrons is less than that for the other field alignment. Also, the range of the energies of the created positrons is much narrower than for the two cases above. Most importantly, we find also here a good match with the scattering data.

We note that the total energy integral over N(E,t) corresponds to the total number of created particles N(t). Due to the excellent match for each energy, the creation rate can therefore also be obtained from the final areas of the transmitted Gaussian wave packets. While the application of Hund's rule to time-independent force fields is well-known and time-dependent forces fields can be described by other techniques [see for example 41, 42], the fact that Hund's rule can be generalized to time-dependent interactions is, to the best of our knowledge, not reported in the literature.

5. Effect of the laser fields and their polarization on the pair creation yield

In this section, we will exploit the prior finding that the vacuum decay process can be mapped onto a scattering problem to obtain a better physical understanding of the laser-assisted pair creation process. We will first examine how the direction of the polarization of an external linearly polarized electric field relative to the static force direction will affect the pair creation process. For the perpendicularly aligned field $A_y(t)$ we can even provide a fully analytical theory for the laser-modified rate $\Gamma(E_0,\omega)$ based on the concept of the relativistic mass shift that proofs that any field will *always reduce* the yield. For the parallel aligned field $A_x(t)$, due to the possibility of multiple photon emission and absorption, the situation seems to be more complicated.

5.1 Analytical expressions for the rate Γ from the scattering theory for A=0

As we have illustrated in Figure 3, the final area $A_{fin}(E)$ of the Gaussian wave packet as a function of the incoming energy plays a key role in determining the vacuum decay. As we have shown in the appendices, in the absence of any laser field this final area is identical to the transmission coefficient for a particle of effective mass M in the same field. It is well known that an analytical expression for this coefficient [30,33,38] is given by

$$T(E;M) = -\sinh[\pi pw]\sinh[\pi kw] / \{\sinh[\pi(|V_0|/c+p+k)w/2]\sinh[\pi(|V_0|/c-p-k)w/2]\} \qquad (5.1)$$

where the two momenta $k = -[(E-|V_0|)^2 - M^2c^4]^{1/2}/c$ and $p = [E^2 - M^2c^4]^{1/2}/c$ depend on the effective mass M.

Using this analytical expression for the special case of laser-free scattering, where the particle's mass is that of the free electron, M=m=1.a.u., we can determine numerical value of the integral $\Gamma = 1/(2\pi) \int dE\, T(E)$, which amounts to Γ=327.591. As discussed in Sec. 4.1, this value is (within our numerical accuracy) identical to the vacuum decay rate Γ read off the graph for N(t) in Figure 2.

5.2 Analytical expressions for the vacuum decay rate Γ from scattering theory for $A_y \neq 0$

For the situation where the laser is polarized along the y-direction, i.e. $\mathbf{E}(\mathbf{r},t) = E_0 \cos(\omega t)\, \mathbf{e}_y$, it is still possible to construct a laser-modified transmission coefficient, which will then lead to an analytical expression for the pair creation rate.

While in a non-relativistic limit ($c \to \infty$) the motion along the three spatial directions is completely decoupled, in a relativistic system an external field pointing in the y-direction, such as $A_y(t)$, affects also the motion along the x-direction. This can be easily seen for the scalar model Hamiltonian $H = [m^2c^4 + c^2p_x^2 + A_y^2(t)]^{1/2}$, where we have chosen the conserved momenta $p_z = p_y = 0$. Here the velocity $v_x = dH/dp_x$ amounts to $v_x = c^2 p_x [m^2c^4 + c^2p_x^2 + A_y^2(t)]^{-1/2}$, which shows that the force associated with $A_y^2(t)$ along the y-direction *always* reduces the velocity v_x. For example, if we consider the oscillatory vector potential $A_y(t) = -E_0 \sin(\omega t)\, c/\omega$ and expand v_x in powers of 1/c, we obtain $v_x = p_x - [p_x^3 + p_x (E_0^2/\omega^2) \sin^2(\omega t)]/(2c^2) + O(c^{-4})$. If we average this expression over one laser period [$\omega/(2\pi) \int dt \sin^2(\omega t) = 1/2$], we find that the laser field along the y-direction reduces the speed along the x-direction by the amount $p_x E_0^2/(4c^2\omega^2)$.

Similarly, and even more relevant, we can also follow earlier works [43-45] and introduce an effective radiative mass m*, defined by the temporal average $m^*(E_0, \omega) \equiv \langle [m^2 + A_y^2(t)/c^4]^{1/2} \rangle$, where $\langle \ldots \rangle$ represents the average over one laser period. More concretely, if we assume $A_y(x,t) = -E_0\, c \sin(\omega t)/\omega$, this average mass amounts to

$$m^*(E_0,\omega) = (2\pi/\omega)^{-1} \int dt \;\; [m^2 + [E_0/(\omega c)]^2 \sin^2(\omega t)]^{1/2} \qquad (5.2)$$

where the integration limits cover one period of the external field, $2\pi/\omega$. We can immediately see that this mass m* depends only on the dimensionless ratio of the non-relativistic ponderomotive energy $E_0^2/(m\omega^2)$ and the electron's rest mass energy mc^2, i.e. $m^*(E_0,\omega) = m\, F[E_0/(mc\omega)]$, where F is the function given by Eq. (5.2). While there is no useful analytical solution of this complete elliptic integral of the second kind, we can at least find the nonrelativistic limit. Using the large-c expansion $\left[m^2 + [E_0/(\omega c)]^2 \sin^2(\omega t)\right]^{1/2} = m + E_0^2/(2m\omega^2c^2) \sin^2(\omega t) + O(c^{-4})$, we can perform the average, leading to $m^*(E_0, \omega) = m + E_0^2/(4m\omega^2c^2) + O(c^{-4})$. For our numerical parameters for the field, we obtain here $m^*(E_0, \omega) = 1.04$ a.u., which compares well with the exact value $m^*(E_0, \omega) = 1.03887364$ a.u. obtained from Eq. (5.2).

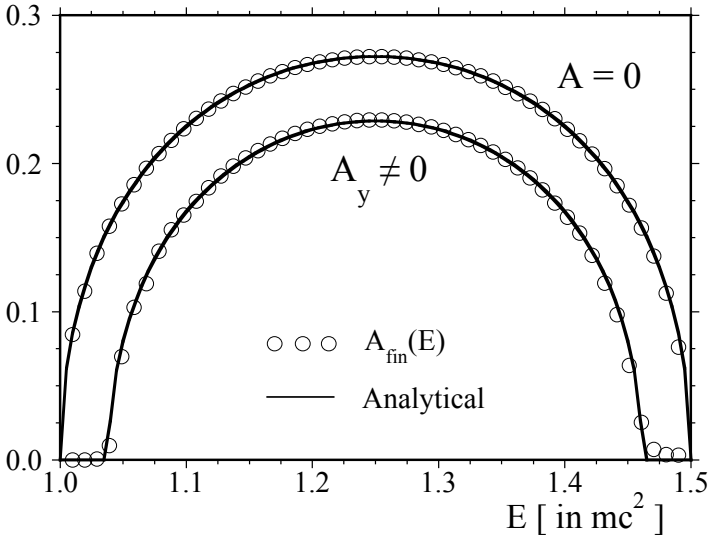

Figure 4 The analytical prediction for the (normalized) energy spectrum of the created electrons, $N(E,t)\, 2\pi/t = \Gamma(E_0,\omega)$ without (top data) and with the time-periodic field $\mathbf{A}(x,t) = -E_0\, c \sin(\omega t)/\omega\, \mathbf{e_y}$ (bottom data). For comparison, the open dots are the numerically obtained final areas $A_{fin}(E)$ of the transmitted portion of the scattered Gaussian wave packet. (same numerical parameters as in Fig.2)

In order to test the accuracy of this analytical prediction, we have compared in Figure 4 the corresponding analytical predictions for the normalized energy spectrum of the created particles $N(E,t)\, 2\pi/t$, which is given by the transmission coefficient $T[E;m^*(E_0, \omega)]$ and based on the laser intensity and frequency dependent mass $M=m^*$ from Eqs. (5.1) and (5.2), with the numerically obtained final areas $A_{fin}(E)$ of the Gaussian wave packet from Figure 3. The agreement is excellent, which shows again that the laser-induced pair creation process for a laser field that is perpendicular to the static field can be mapped rather exactly onto a scattering problem where the particle has an

effective mass m* given by Eq. (5.2).

The relativistic increase of the effective mass also explains the observed symmetric narrowing of the permitted energy range of the created particles in Fig. 3. While in the absence of any laser this range extends from $E = mc^2$ to $|V_0| - mc^2$, the laser modified range is only $m^*(E_0,\omega)c^2$ to $|V_0| - m^*(E_0,\omega)c^2$. Using the non-relativistic expansion of $m^*(E_0,\omega)$ from above suggests that the observed energy range for N(E,t) narrows with increasing field strength E_0 and decreasing ω.

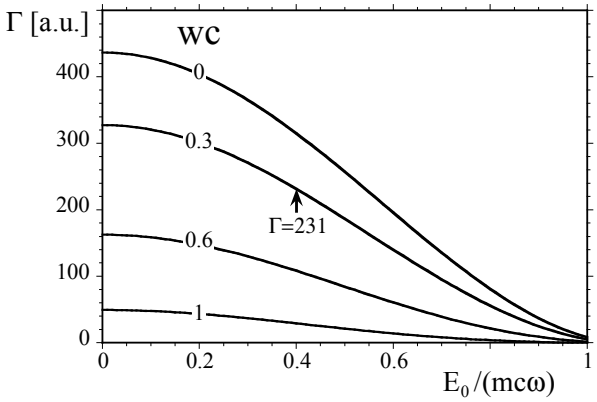

Figure 5 The analytical prediction for the laser-assisted vacuum decay rate $\Gamma(E_0,\omega)$ [from Eqs. (5.1) and (5.2)] as a function of the scaled laser amplitude $E_0/(mc\omega)$ for four spatial extensions of the static supercritical field with amplitude $V_0 = -2.5mc^2$. The arrow marks the parameter used in Figs. 2b,3 and 4.

As a last and final step, we can now use this analytical expressions Eq. (5.1) and (5.2) to estimate the laser-assisted vacuum decay rate according to

$$N(t)/t = \Gamma(E_0,\omega) = 1/(2\pi) \int dE\, T[E;m^*(E_0,\omega)] \qquad (5.3)$$

For example, for the numerical parameters ($E_0=0.2c^3$, $\omega= 0.5mc^2$) used in Figs. 2b, 3 and 4, this integral amounts to $\Gamma(E_0,\omega) = 231.272$, which matches very well the observed averaged slope in Fig. 2b. To obtain a more general idea as to how this rate decreases with the dimensionless parameter $E_0/(mc\omega)$ for m=1 a.u., we have graphed in Figure 5 the vacuum decay rate $\Gamma(E_0,\omega)$ for several spatial extensions w of the static supercritical field.

We can also use this analytical expression to study the scaling of the rate $\Gamma(E_0,\omega)$ with the laser parameters. If we assume for simplicity that the static field is very narrow ($w\rightarrow 0$), Eq. (5.1)

simplifies to $N(E,t)\,2\pi/t = -4pk/\{(V_0^2/c^2-(p+k)^2\}$. This takes the largest value for the energy $E^*=V_0/2$, for which $p=-k$. The resulting expression simplifies to $N(E^*,t)\,2\pi/t = 1-4\,M^2/(V_0/c^2)^2$. If we insert expansion for $M= m^*(E_0,\omega) = m + E_0^2/(4m\omega^2c^2) + O(c^{-4})$ we obtain

$$N(E^*,t) = N_{E0=0}(E^*,t) - t\,[E_0/(\omega c)]^2\,/\pi \qquad (5.4)$$

This means that the reduction of the number of created particles does not depend on V_0 of the static field. If we assume that the integrand in the expression for $N(t) = \int dE\, N(E,t)$ can be approximated by its largest value, the integral over the range from $E = m^*c^2$ to $|V_0| - m^*c^2$, can be evaluated as

$$\begin{aligned} N(t) &\approx (|V_0| - 2\,m^*c^2)\ \{N_{E0=0}(E^*,t) - t\,[E_0/(\omega c)]^2\,/\pi\} \\ &\approx [|V_0| - 2\,(mc^2 + E_0^2/(4m\omega^2)]\ \{N_{E0=0}(E^*,t) - t\,[E_0/(\omega c)]^2/\pi\} \end{aligned} \qquad (5.5)$$

We see that the overall laser-induced reduction of the total number of created particles is due to a decrease associated with the energy density for each energy [Eq. (5.4)] as well as a decrease of the energy range at which the particles occur.

6. Effect of laser's spatial inhomogeneity on yield

For conceptual simplicity, so far we have modeled the laser field above only by a spatially homogeneous alternating electric field and therefore neglected the effect of any spatial dependence and possibly its magnetic field component. In order to outline future challenges, we will examine briefly in this section this effect by comparing the energy spectra of the created positronss $N(E,t)$ from the above sections with those obtained from the laser fields given by the vector potentials $\mathbf{A}(x,t) = E_0\,\sin(\omega t-kx)\,\mathbf{e}_x$ and $\mathbf{A}(x,t) = E_0\,\sin(\omega t-kx)\,\mathbf{e}_y$.

In Figure 6 we have displayed the scaled data $N(E,t)\,2\pi/t$. For the laser field polarized along the y-direction (right figure), the yield is indistinguishable from that obtained for spatially homogeneous field for all energies and the radiative mass increase governs the laser-assisted decrease of the pair creation yield. Here the corresponding time-dependent magnetic field, $\mathbf{B}(x,t) = dA_y/dx\,e_z$, points in the z-direction and apparently does not affect the pair creation process.

On the other hand, for the vector potential along the x-direction (left figure) the impact of its

spatial dependence is much more interesting. It has a dramatic and rather non-trivial effect on the spectrum that depends on the energy of the created electrons, as some energies are enhanced and others reduced compared to the laser-free case as well as to the case where kx=0. While this particular field configuration has no magnetic field component, as $\nabla \times \mathbf{A} = 0$, the impact of the kx term in $\mathbf{A}(x,t)$ affects only the corresponding electric field, $\mathbf{E}(x,t) = -c^{-1}\,\partial\mathbf{A}/\partial t - \nabla V(x)$ in the direction of the static force field. As this direction is more relevant for the pair creation, any modification of the term $\partial\mathbf{A}/\partial t$ has a measurable impact on the yield.

We should mention that also for both external fields with $kx \neq 0$ the data are perfectly matched with the Gaussian scattering data. We have to point out that due to the projection on field-free states, one should not overinterpret the time-dependence of the yield $N(t) = \int dE\, N(E,t)$ during the interaction time. The observed rapid oscillations with frequency 2ω shown in Figure 2 are almost suppressed for both polarization directions when the laser field has a spatial as well as time dependence. Here we observe a nearly monotonic increase of N(t) during the plateau region of the external fields.

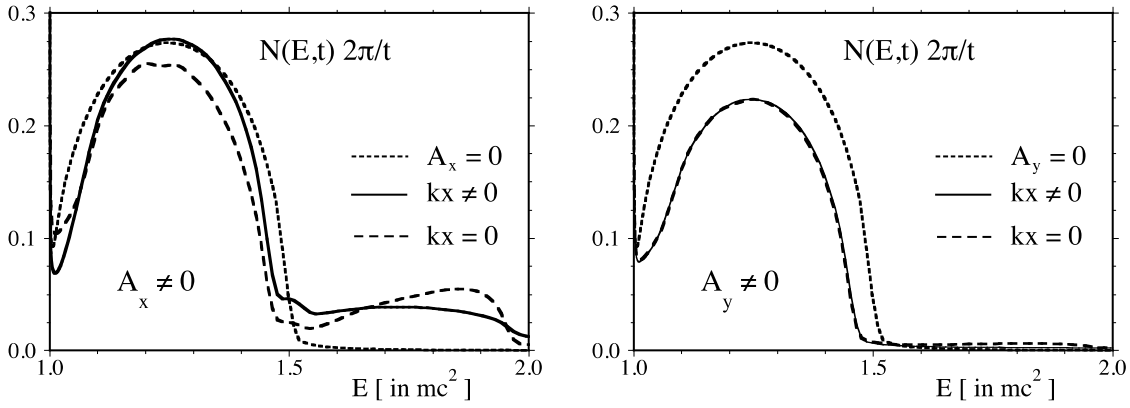

Figure 6 Comparison of the energy spectra of the created particles from the laser-assisted pair creation process with and without the effect of the magnetic field component, N(E,t) $2\pi/t$ for the field polarized parallel (left) and perpendicular (right) to the static force. The dotted line is the spectrum without any laser field. (Parameters as in Fig. 2).

7. Summary and open questions

We have suggested that it is possible to map the quantum field theoretical problem of the decay of the QED vacuum state onto the quantum mechanical problem of laser-assisted scattering where the incoming scattering particle is comprised of negative energy states of the force-free Dirac

equation. We should note here a rather peculiar feature of the relationship between the energies involved in the scattering and the corresponding vacuum decay. The mapping is non-trivial as the absolute value of the (chosen) *initial* energy of the incoming wave packet is identical to the *final* energy of the created positron in the vacuum decay process even in the case of laser-induced energy transitions. The total energy of the incoming wave packet's energy (comprised of Dirac states) is actually positive due to the "lift" by the external potential energy $|V_0|$. In the absence of any laser this energy is conserved. However, in the presence of the laser field, the energy of the wave packet is not conserved due to multi-photon transitions, such that the final scattered state can contain several energies. It is noteworthy that also in the laser-assisted decay the chosen *initial* energy (and *not* the final one) matches that of the created positron.

While this equivalence opens the door to new theoretical approaches, one might also wonder if it is even possible to model this process in classical mechanical terms of relativistic scattering [46] similar to those established for laser-assisted scattering [14-20]. It was suggested that some of the features of quantum mechanical interactions, such as self-repulsion [47], energy spectra in pair creation [48], and relativistic resonances [49,50] can indeed be reproduced with surprising accuracy by corresponding classical ensembles of quasi-particles. We presently certainly lack any classical intuition for the Klein tunneling through a supercritical barrier. We reiterate that this "scattering" potential is peculiar as the energy of an incoming particle determines whether the particle is accelerated or decelerated. Here it would be required to develop a classical mechanical description that permits "classical" particles to take formally a negative energy. For some early first ideas in this direction, see the works by Costella et al. [51] who suggested how anti-particle motion is not a pre-requisite but can be dealt with in classical mechanics itself. This goal is, of course, very speculative and might also make use of two-state particles or to make physical sense out of particles that formally involve backward in time as suggested by the Feynman-Stueckelberg interpretation [52,53].

In this work, the vacuum state is represented by the complete set of (negative) energy eigenstates, whose temporal evolution had to be obtained by the dynamics of each (Dirac sea) state separately. This tedious task is unfortunately rather computer memory and CPU time consuming and its feasibility often requires a restriction of the spatial dimension. In order to be able to tackle also 3D situations with full space-time resolution, two interesting early works [24,25] proposed to model the quantum field theoretical vacuum state by just a single quantum mechanical state that is a superposition of only a few eigenstates. In Ref. [24] the vacuum was modeled by a single electron

wave packet of negative energy at rest to be sufficiently narrow in momentum, to exclude unphysical interference effects between different momentum states. In [25] a single quantum mechanical state was chosen that included, as a linear superposition, all possible momentum states up to a certain maximum. While these single-state calculations provided us with plenty of new information about multi-photon processes in the context of pair-creation, it should be kept in mind that they nevertheless represent only a certain sub-portion of the Dirac sea. It seems computationally a very promising task to being able to identify apriori, which of the initially occupied Dirac states are dynamically most relevant. The mapping of quantum field theory onto quantum mechanical states discussed in this work might provide a new guidance and avenues for this goal. Complementary to the present computational approach, there has been also some significant progress obtained using real-time lattice techniques [54-56]. These rely on the classical-statistical approximation that is valid in the small coupling limit.

While our approach permitted us to include the laser polarization directions being aligned at arbitrary angles relative to the static electric field vector of the static potential, we note that it was possible here to restrict the spatial domain to only the x-direction, as the canonical momenta in the y and z-direction were conserved. In a more general situation where the spatially dependent external field varies also along the other two directions, more studies will be required.

Acknowledgements

QZL and SD would like to thank ILP for the nice hospitality during their visits to Illinois State. This work has been supported by the German Humboldt Foundation, NSF, the NSFC (#11529402), by Research Corporation and the Strategic Priority Research Program of the Chinese Academy of Sciences (Grant No. XDB16010200).

Appendix A

We will now examine the general expression (3.2) for the special case where the positrons are created solely by a static supercritical field V(x). We will show below that in the long-time limit the energy density grows linearly in time and can be expressed in terms of the quantum mechanical transmission coefficient where the energy E is in the range mc^2 to $|V_0| - mc^2$. Here among all possible initial Dirac states $|k;d\rangle$ only a small subgroup of states happen to contribute to the vacuum decay in the long-time limit. It turns out that only those Dirac sea states that have a negative momentum (due to our choice of sign $V_0<0$), which is in the energy range between $-|V_0| + mc^2 < -[m^2c^4+c^2k^2]^{1/2} < -mc^2$ can contribute in the long-time limit.

As a quick excursion, we have to briefly summarize first some stationary properties of this field configuration. Let us assume that the external force field is localized around x=0 and given by a scalar potential V(x) that fullfils $V(x=-\infty) = V_0$ and $V(x=\infty) = 0$ such as the Sauter potential used in our numerical analysis. The height $|V_0|$ is assumed to be supercritical, i.e., $|V_0| > 2mc^2$. For a given *positive* (auxiliary) energy in the range $mc^2<E_+<|V_0|-mc^2$ there exists a stationary energy eigenstate of the Dirac Hamiltonian that fulfills $[c\sigma_1 p + c^2 \sigma_3 - V(x)] |E_+\rangle = E_+ |E_+\rangle$. This state contains the reflection and transmission amplitudes.

On the right side (x>0) of the potential (where $V(x)\approx 0$) the wave function of this state $|E_+\rangle$ describes an outgoing (right-traveling) electron state $\phi_{tran}^{+}(x,p)$ with a characteristic transmission amplitude τ. If we analytically continue this state to all positions x it would have a (positive) momentum p and energy $E_+ \equiv [m^2c^4+c^2p^2]^{1/2}$, as it would satisfy $[c\sigma_1 p_x + c^2 \sigma_3] \phi_{tran}^{+}(x,p;u) = E_+ \phi_{tran}^{+}(x,p;u)$. The energy-dependence of the transmission amplitude τ depends on the details of the region where the electric field is non-zero and can be obtained by assuming that the asymptotic current densities are the same, i.e., $\mathbf{j}_{inc} + \mathbf{j}_{ref} = \mathbf{j}_{tran}$. The corresponding transmission coefficient is defined by the ratio of the transmitted current and the incoming current, $\equiv \mathbf{j}_{trnas}/\mathbf{j}_{inc} = |\tau|^2 v_{tran}/v_{inc}$, where $v_{trans} = c^2 p /[m^2c^4+c^2p^2]^{1/2}$ and $v_{inc} = c^2 |k|/[m^2c^4+c^2k^2]^{1/2}$.

On the left side of the electric field (x<0), the energy eigenstate is a superposition of an incoming $\phi_{in}^{-}(x,k;d)$ and a reflected $\phi_{ref}^{-}(x,-k;d)$ state, where the *negative* momentum k is related to the auxiliary energy E_+ according to $E_+ = |V_0| - [m^2c^4+c^2k^2]^{1/2}$. It is important to remark, that (after analytic continuation to all positions) both states ϕ_{in}^{-} and ϕ_{ref}^{-} are identical to free-force eigenstates

with *negative* energy, as they both fulfill $[c\sigma_1 p_x + c^2\,\sigma_3]\,\phi^-(x,\pm k;d) = (E_+ - |V_0|)\,\phi^-(x,\pm k;d)$. As characteristic of all eigenstates with negative energy, a negative momentum k corresponds to a positive current density presenting a particle moving to the right.

After this excursion to stationary scattering theory, we can now return to the interpretation of the evolution of the spatial density $\rho_k(x,t)$. At the initial time, this density $\rho_k(x,t)$ vanishes identically and it would remain so for all times in the absence of any forces, V'(x)=0. This means that any spatial growth of $\rho_k(x,t)$ can occur only at those specific spatial regions where the force V'(x) is nonzero. This means that any non-vanishing portion of $\rho_k(x,t)$ originates close to x=0 and then consecutively could propagate into the positive and (at least in principle) into the negative x-direction. The initial Dirac state $|k;d\rangle$ with *negative* energy $-[m^2c^4+c^2k^2]^{1/2}$ and negative momentum k has the largest overlap (scalar product) with the specific scattering state $|E_+\rangle$ that has the (auxiliary) *positive* energy $E_+ = |V_0| - [m^2c^4+c^2k^2]^{1/2}$. This should be obvious as the two wave functions $\phi_{in}^-(x,k;d)$ and $\langle x|k;d\rangle$ are identical under the barrier V(x).

This means we have arrived at the following visual picture. The population associated with the initial state $|k;d\rangle$ "flows" to the region x≈0, where it is continuously converted to a state $\phi_{tran}^+(x,p;u)$ that "flows" out to the right with momentum p. For sufficiently long times, we can now calculate the integral $\int dx\ \rho_k(x,t)$ by the product of the height of $\rho_k(x,t)$ and its spatial extension.

The height of $\rho_k(x,t)$ follows from the fact that $|k;d\rangle$ mainly excites $|E_+\rangle$. In other words, its amplitude should match that of $|\phi_{tran}^+(x,p;u)|^2$, which is $|\tau(E_+)|^2/L$ Here the second factor is the result of the (finite) total length L of our system and a direct consequence of the box normalization of all states $\langle k_1;d|k_2;d\rangle = \delta_{k1,k2}$ as mentioned in Sec. 2. The length of the spatial region [where $\rho_k(x,t) = 1/L\ |\tau(E_+)|^2 \neq 0$] is given by the product of the velocity and time, i.e., $v_{tran}\,t$. As a result, we can estimate

$$\int dx\ \rho_k(x,t) = 1/L\ |\tau(E_+)|^2\ v_{trans}\,t \qquad (A.1)$$

If we introduce the transmission coefficient via the expression $|\tau(E_+)|^2\ v_{tran} = T(E_+)\ v_{inc}$, we obtain $N_k(t) = \int dx\ \rho_k(x,t) = 1/L\ T(E_+)\ v_{inc}\,t$. If we convert the (discrete) density $N_k(t)$ to the corresponding energy density (as outlined in Sec. 2.4 above), we obtain

$$N(E,t) = (2\pi)^{-1}\, T(E_+)\, t \;=\; (2\pi)^{-1}\, T(|V_0|-E)\, t \qquad (A.2)$$

as the velocity term as well as the numerical box size L cancels out.

Appendix B

In this appendix, we will show that for general static electric field configurations for which the corresponding electric field is even (symmetric) with respect to a given location, the transmission coefficient is symmetric with regard to its central energy $|V_0|/2$, i.e. $T(|V_0|-E) = T(E)$. This proof relies on the existence of the anti-unitary charge conjugation operator C, which for the Hamiltonian (2.1) in the (standard-Dirac) representation takes the form $C=i\beta\alpha_2K$, where K is the (anti-linear) complex conjugation operator. For the Hamiltonian (2.2) it takes the analogous, but simpler form $C = i\,\sigma_3\sigma_2K = \sigma_1K$. It should not be confused with the (more important) quantum field theoretical operator. It has the property that any general Hamiltonian for an electron of charge q coupled to an external field, i.e., $H(q) \equiv H_0 - q\,\boldsymbol{\alpha}\mathbf{A} + qV$, can be transformed into the corresponding Hamiltonian for a positron coupled to the same field, i.e. $CH(q)\,C = -H(-q)$.

If we apply this operator on both sides of the eigenvalue equation for the stationary scattering state $(H_0+qV)\,|E_+\rangle = E_+\,|E_+\rangle$ (discussed in Appendix A), we obtain

$$C\,(H_0+qV)\,C\,C\,|E_+\rangle \;=\; C\,E_+\,|E_+\rangle \qquad (B.1)$$

where we also have inserted the unit operator $C\,C = 1$. Using the charge conjugation symmetry $CH(q)\,C = -H_0 + qV(x)$, subtracting the constant positive energy $qV_0 = |V_0|$ on both sides of the equation, and multiplying with -1, we obtain

$$[H_0 - qV(x) + qV_0]\,C\,\phi(x) \;= (qV_0 - E_+)\;C\phi(x) \qquad (B.2)$$

The original wave function $\phi(x)$ was a scattering eigenstate with energy E_+ associated the potential $V(x)$ with the asymptotic properties $V(-\infty) = V_0$ and $V(\infty) = 0$ corresponding to an incoming

particle from the left (k<0) with the asymptotic properties state $\phi(x) = \langle x|k;d\rangle + r\langle x|{-}k;d\rangle$, where $V(x)=V_0$. For positive x [where V(x)=0] the state represented the transmitted portion, given by $\phi(x) = t\langle x|p;u\rangle$. Eq. (B.2) shows that the wave function $C\phi(x)$ is an eigenstate of the Hamiltonian $H_0+qW(x)$, where the new potential $W(x) = -V(x) + V_0$ has the *identical* shape as V(x), it is just reversed with regard to its asymptotic properties, i.e. $W(-\infty) = 0$ and $W(\infty) =V_0$. However, the wave function $C\phi(x)$ has the different energy qV_0-E_+.

The charge conjugation operation changes the signs of the momenta and reverses basically the role of upper and lower energy states. As a result, $C\phi(x)$ is a superposition of the incoming and reflected state, $C\phi(x) = \langle x|{-}k;u\rangle + r^* \langle x|k;u\rangle$ [for the left region where W(x) =0] and the transmitted portion $C\phi(x) = \tau^* \langle x|{-}p;d\rangle$ for the right region where $W(x) =V_0$. Therefore $\phi(x)$ and $C\phi(x)$ contain the transmission coefficients that are just complex conjugates of each other, even though they are associated with different energies E_+ and qV_0-E_+ and different potentials V(x) and W(x).

In general, the associated potentials V(x) and W(x) are different from each other. However, the situation is different if the electric field has some symmetry under spatial inversion. For example, V'(x) = V'(–x) can lead to $V(-x) = -V(x) + V_0$ and we obtain W(–x) = V(x). This means that the spatially inverted solutions $C\phi(-x)$ and $\phi(x)$ are both solutions associated with the same potential V(x), but energies E_+ and qV_0-E_+. This means that we have proven the symmetry property $T(E_+) = T(qV_0 - E_+)$ such that Eq. (A.2) simplifies to

$$N(E,t) = (2\pi)^{-1} T(E)\, t \qquad (B.3)$$

References

[1] For recent advances, see, e.g. https://eli-laser.eu/

[2] For a comprehensive review, see A. Di Piazza, C. Müller, K.Z. Hatsagortsyan and C.H. Keitel, Rev. Mod. Phys. 84, 1177 (2012).

[3] J.S. Schwinger, Phys. Rev. 128, 2425 (1962).

[4] For early work, see G. Breit and J.A. Wheeler, Phys. Rev. 46, 1087 (1934).

[5] H.R. Reiss, J. Math. Phys. 3, 59 (1962); Phys. Rev. Lett. 26, 1072 (1971).

[6] W. Greiner, B. Müller and J. Rafelski, "Quantum electrodynamics of strong fields" (Springer Verlag, Berlin, 1985).

[7] F. Hund, Z. Phys. 117, 1 (1941).

[8] A. Hansen and F. Ravndal, Phys. Scr. 23, 1036 (1981); N. Dombey and A. Calogeracos, Phys. Rep. 315, 41 (1999).

[9] P. Krekora, K. Cooley, Q. Su and R. Grobe, Phys. Rev. Lett. 95, 070403 (2005).

[10] R.E. Wagner, M.R. Ware, Q. Su and R. Grobe, Phys. Rev. A 81, 052104 (2010).

[11] W. Su, M. Jiang, Q.Z. Lv, Y.J. Li, Z.M. Sheng, R. Grobe and Q. Su, Phys. Rev. A 86, 013422 (2012).

[12] F. Fillion-Gourdeau, E. Lorin and A.D. Bandrauk, Phys. Rev. Lett. 110, 013002 (2013).

[13] Q. Su, W. Su, Q.Z. Lv, M. Jiang, X. Lu, Z.M. Sheng and R. Grobe, Phys. Rev. Lett. 109, 253202 (2012).

[14] N.M. Kroll and K.M. Watson, Phys. Rev. A 8, 804 (1973).

[15] H. Krüger and C. Jung, Phys. Rev. A 147, 1706 (1978).

[16] J. Banerji and M.H. Mittleman, J. Phys. B 14, 3717 (1981).

[17] P.S. Krstic and D.B. Milosevic, J. Phys. B 20, 3487 (1987).

[18] F.H.M Faisal, "Theory of multi-photon processes" (Springer Verlag, Heidelberg, 1987).

[19] L.B. Madsen and K. Taulbjerg, J. Phys. B 28, 5327 (1995).

[20] A. Jaron and J.Z. Kaminski, Laser Phys. 9, 81 (1999).

[21] A. Weingartshofer, J.K. Holmes, J. Sabbagh and S.L. Chin, J. Phys. B 16, 1805 (1983).

[22] B. Wallbank and J.K. Holmes, Phys. Rev. A 48, R2515 (1993).

[23] B. Wallbank and J.K. Holmes, J. Phys. B 27, 1221 (1994).

[24] M. Ruf, G.R. Mocken, C. Müller, K. Z. Hatsagortsyan and C.H. Keitel, Phys. Rev. Lett. 102, 080402 (2009).

[25] G.R. Mocken, M. Ruf, C. Müller and C.H. Keitel, Phys. Rev. A 81, 022122 (2010).

[26] Q.Z. Lv, S. Dong, Y.T. Li, Z.M. Sheng, Q. Su and R. Grobe, Phys. Rev. A (submitted).
[27] B. Thaller, "The Dirac Equation" (Springer, Berlin, 1992).
[28] T. Cheng, Q. Su and R. Grobe, Cont. Phys. 51, 315 (2010).
[29] B.S. Xie, Z.L. Li, S. Tang, Matter and Radiation at Extremes 2, 225 (2017).
[30] F. Sauter, Z. Phys. 69, 742 (1931).
[31] M.D. Feit, J.A. Fleck, Jr., and A. Steiger, J. Comput. Phys. 47, 412 (1982).
[32] A.D. Bandrauk, H. Shen, J. Chem. Phys 99, 1185 (1993).
[33] J.W. Braun, Q. Su and R. Grobe, Phys. Rev. A 59, 604 (1999).
[34] W. Su, M. Jiang, Z.Q. Lv, Y.J. Li, Z.M. Sheng, R. Grobe and Q. Su, Phys. Rev. A 86, 013422 (2012).
[35] M. Jiang, W. Su, Z.Q. Lv, X. Lu, Y.J. Li, R. Grobe and Q. Su, Phys. Rev. A 85, 033408 (2012).
[36] Q.Z. Lv, A.C. Su, M. Jiang, Y.J. Li, R. Grobe and Q. Su, Phys. Rev. A 87, 023416 (2013).
[37] S.S. Dong, M. Chen, Q. Su and R. Grobe, Phys. Rev. A 96, 032120 (2017).
[38] R. Schützhold, H. Gies and G. Dunne, Phys. Rev. Lett. 101, 130404 (2008).
[39] M. Orthaber, F. Hebenstreit and R. Alkofer, Phys. Lett. B 698, 80 (2011).
[40] E. Brezin and C. Itzykson, Phys. Rev. D 2, 1191 (1970).
[41] V.S. Popov, Sov. Phys. JETP 35, 659 (1972).
[42] T. Cheng, M. Ware, Q. Su and R. Grobe, Phys. Rev. A 80, 062105 (2009).
[43] L.S. Brown and T.W.B. Kibble, Phys. Rev. 133, A705 (1964).
[44] J.H. Eberly and A. Sleeper, Phys. Rev. 176, 1570 (1968).
[45] C. Kohlfürst, H. Gies and R. Alkofer, Phys. Rev. Lett. 112, 050402 (2014).
[46] R.E. Wagner, P.J. Peverly, Q. Su and R. Grobe, Las. Phys.11, 221 (2001).
[47] Q.Z. Lv, S. Norris, Q. Su and R. Grobe, Phys. Rev. A 90, 034101 (2014).
[48] N.I. Chott, Q. Su and R. Grobe, Phys. Rev. A 76 010101 (R) (2007).
[49] R.E. Wagner, Q. Su and R. Grobe, Phys. Rev. Lett 84, 3282 (2000).
[50] R.E. Wagner, P.J. Peverly, Q. Su and R. Grobe, Phys. Rev. A. 61, 35402 (2000).
[51] J.P. Costella, B.H.J. McKellar and A.A. Rawlinson, Am. J. Phys. 65, 835 (1997).
[52] E. Stueckelberg, Helv. Phys. Acta 14, 322 (1941).
[53] R.P. Feynman, Rev. Mod. Phys. 20, 367 (1948).
[54] V. Kasper, F. Hebenstreit and J. Berges, Phys. Rev. D 90, 025016 (2014).
[55] N. Mueller, F. Hebenstreit and J. Berges, Phys Rev. Lett. 117, 061601 (2016).

[56] P.V. Buividovich and M.V. Ulybyshev, Phys. Rev. D 94, 025009 (2016).